

Adaptive Trotterization for Time-Dependent Hamiltonian Quantum Dynamics Using Piecewise Conservation Laws

Hongzheng Zhao^{1,2,3,*}, Marin Bukov⁴, Markus Heyl^{4,5}, and Roderich Moessner⁴


¹*School of Physics, Peking University, 100871 Beijing, China*

²*Max Planck Institute for the Physics of Complex Systems, Nöthnitzer Straße 38, 01187 Dresden, Germany*

³*Institute for Quantum Optics and Quantum Information, Technikerstraße 21a, 6020 Innsbruck, Austria*

⁴*Max Planck Institute for the Physics of Complex Systems, Nöthnitzer Straße 38, 01187 Dresden, Germany*

⁵*Theoretical Physics III, Center for Electronic Correlations and Magnetism, Institute of Physics, University of Augsburg, 86135 Augsburg, Germany*

 (Received 26 July 2023; revised 31 March 2024; accepted 30 May 2024; published 2 July 2024)

Digital quantum simulation relies on Trotterization to discretize time evolution into elementary quantum gates. On current quantum processors with notable gate imperfections, there is a critical trade-off between improved accuracy for finer time steps, and increased error rate on account of the larger circuit depth. We present an adaptive Trotterization algorithm to cope with time dependent Hamiltonians, where we propose a concept of *piecewise “conserved” quantities* to estimate errors in the time evolution between two (nearby) points in time; these allow us to bound the errors accumulated over the full simulation period. They reduce to standard conservation laws in the case of time independent Hamiltonians, for which we first developed an adaptive Trotterization scheme [H. Zhao *et al.*, Making Trotterization adaptive and energy-self-correcting for NISQ devices and beyond, *PRX Quantum* **4**, 030319 (2023)]. We validate the algorithm for a time dependent quantum spin chain, demonstrating that it can outperform the conventional Trotter algorithm with a fixed step size at a controlled error.

DOI: [10.1103/PhysRevLett.133.010603](https://doi.org/10.1103/PhysRevLett.133.010603)

Introduction.—Simulating the time evolution of nonequilibrium quantum many-body systems poses a significant challenge for classical computers due to the exponentially large Hilbert space dimension [1,2]. The rapid development of quantum processors holds the promise of resolving this key problem through digital quantum simulation (DQS) [3–11].

In DQS, the continuous time evolution operator is discretized into elementary few-body quantum gates, a procedure known as Trotterization [12–29]. However, due to their noncommutativity, Trotterization introduces errors, which can accumulate over longer simulation times. While a finer Trotter time step size δt improves simulation precision, it also leads to increased circuit depth. In the current era of noisy intermediate-scale quantum (NISQ) processors, gate imperfections are inevitable, posing a significant challenge in improving the accuracy of DQS [2], especially in the absence of experimentally efficient error-correction schemes [30–32]. Therefore, it is crucial to identify strategies for minimizing circuit depth while keeping the simulation error under control.

In previous work [33], we introduced a quantum algorithm, ADA-Trotter, allowing for adaptive step sizes δt to optimize the usage of quantum gates for time *independent* Hamiltonians. By measuring the expectation values of energy and energy variance, δt is maximized as long as errors in these conserved quantities remain bounded. According to the central limit theorem, ADA-Trotter ensures a correct energy distribution for generic nonintegrable many-body systems. However, extending this formalism to time dependent Hamiltonians $H(t)$ is a demanding challenge, since: (i) Energy conservation is absent and hence it is *a priori* unclear how to define a criterion to adapt δt ; (ii) without a static reference Hamiltonian the energy distribution is difficult to define, and hence the implication of the central limit theorem, mentioned above, is now elusive; (iii) generic many-body systems absorb energy from time dependent modulations and may heat up (in the sense of the eigenstate thermalization hypothesis [34,35]) and eventually approach states with trivial correlations [36–38]. It is not clear how to control the additional heating generated by the piecewise constant time dependence of a Trotterized Hamiltonian compared to that of $H(t)$.

In this Letter, we propose tADA-Trotter—an adaptive algorithm for time dependent quantum systems [39–46]. To achieve this, we first discretize the time evolution into small time intervals $[t, t + \delta t]$. In each interval, the time evolution can be generated by an effective Hamiltonian $H_{[\infty]}^{t, \delta t}$. Note

Published by the American Physical Society under the terms of the *Creative Commons Attribution 4.0 International* license. Further distribution of this work must maintain attribution to the author(s) and the published article’s title, journal citation, and DOI. Open access publication funded by the Max Planck Society.

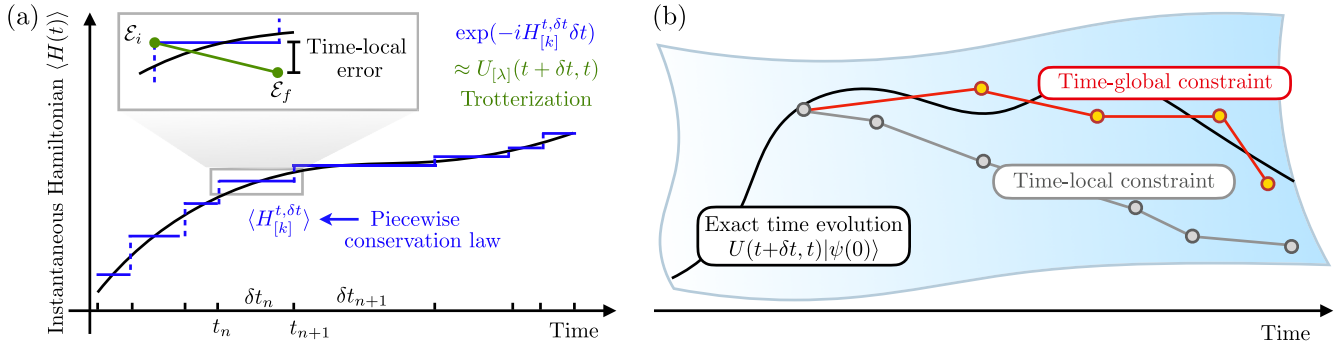


FIG. 1. Schematics of tADA-Trotter for a time dependent Hamiltonian. (a) The expectation values of the piecewise conserved Hamiltonian $H_{[\infty]}^{t, \delta t}$ coincide at times t and $t + \delta t$. The exact expectation value of $H(t)$ is depicted as black line. We use a Magnus expansion to approximate this conservation law $H_{[\infty]}^{t, \delta t} \approx H_{[k]}^{t, \delta t}$ (blue) and a Trotter decomposition (green) for the time evolution. Both approximations introduce errors to the time evolution. We maximize δt as long as errors in this conservation law are bounded, i.e., deviations in the expectation value before (\mathcal{E}_i) and after (\mathcal{E}_f) the Trotterized evolution (green) should be small. (b) Schematic depiction of state space, showing the exact time evolution (black line), as well as the approximate state vector evolution calculated using tADA-Trotter under either time local (gray-black circles) or time global (orange-red circles) constraints. Trotter errors accumulate with the time local constraint (gray), $|\mathcal{E}_f(t_n, \delta t_n) - \mathcal{E}_i(t_n, \delta t_n)| < d_{\mathcal{E}}$. This can be suppressed by using the time global (accumulated) constraint (red), $|\sum_n [\mathcal{E}_f(t_n, \delta t_n) - \mathcal{E}_i(t_n, \delta t_n)]| < d'_{\mathcal{E}}$, leading to more reliable simulation with adaptive step sizes.

that this Hamiltonian has only a parametric dependence on t , δt ; it is time independent once t and δt are fixed. Consequently, the expectation values of $H_{[\infty]}^{t, \delta t}$ and its higher moments coincide at the boundaries of this time window for perfect time evolution, a feature we will refer to as *piecewise conservation laws*, cf. Fig. 1(a). In practice, $H_{[\infty]}^{t, \delta t}$ can be approximated using a perturbative Magnus expansion in the small time step δt [47,48]. The Magnus and Trotterization approximations introduce errors in the piecewise conservation laws. Our key finding is that, by constraining these errors, the step size can be adapted to reduce circuit depth while maintaining a given simulation accuracy for generic nonintegrable many-body systems.

The adaptive step size is determined by measuring piecewise conservation laws using Trotterized time evolution. Subsequently, we introduce the concept of a *time global error*, which represents the accumulation of time local errors in the piecewise conservation laws, cf. Fig. 1. To adapt the step size, we propose a feedback procedure that can bound both the local and global errors.

Notably, Trotter-induced heating effects present in a local control scheme, where simulation errors significantly accumulate over time by making suboptimal choices of δt , may be efficiently suppressed by imposing constraints on the global errors, cf. Fig. 1(b). For time independent systems, this globally constrained scheme reduces to the algorithm proposed in Ref. [33], enabling strict error bounds throughout the entire time evolution. To determine the advantages of a globally constrained error, we perform numerical simulations of a quantum spin chain with a time dependent field. We also demonstrate that tADA-Trotter outperforms the conventional fixed-step Trotter, as depicted

in Fig. 4. These findings highlight the superior potential of tADA-Trotter with a global constraint in minimizing circuit depth for DQS of time dependent systems.

Piecewise conservation laws.—The time evolution operator $U(t, t')$ follows the equation $\partial_t U(t, t') = -iH(t)U(t, t')$, where $H(t)$ represents the time dependent Hamiltonian. Its solution is given by the time ordered exponential $U(t + \delta t, t) = \mathcal{T} \exp(-i \int_t^{t+\delta t} H(s) ds)$, and the exact state evolves as $|\phi(t + \delta t)\rangle = U(t + \delta t, t)|\phi(t)\rangle$.

Formally rewriting $U(t + \delta t, t) = \exp(-iH_{[\infty]}\delta t)$ indicates that the same time evolution can be generated by the static effective Hamiltonian $H_{[\infty]}$, where we drop its parametric dependence on t , δt for simplicity. Hence, when t and δt are fixed, the expectation value of $H_{[\infty]}$, and its higher-order moments, coincide for the states $|\phi(t + \delta t)\rangle$ and $|\phi(t)\rangle$. We use these piecewise conservation laws to adapt the Trotter step size δt .

The piecewise conserved Hamiltonian can be obtained through a Magnus expansion given by $H_{[\infty]} = i\delta t^{-1} \sum_{n=1}^{\infty} \Omega_n$, where the operator $\Omega_n \propto \delta t^n$. The explicit form of $H_{[\infty]}$ can be complicated as higher-order contributions typically involve nested commutators. To eliminate the time ordered integral in the Magnus expansion, we expand the time dependence in Legendre polynomials, obtaining the concise expression for terms of lowest orders [48]: $\Omega_{2m} = 0$ for all even orders $2m$, and

$$\begin{aligned} \Omega_1 &= A_1, & \Omega_3 &= -\frac{1}{6}[A_1, A_2], \\ \Omega_5 &= \frac{1}{60}[A_1, [A_1, A_3]] - \frac{1}{60}[A_2, [A_1, A_2]] \\ &\quad + \frac{1}{360}[A_1, [A_1, [A_1, A_2]]] - \frac{1}{30}[A_2, A_3], \end{aligned} \quad (1)$$

where each operator $A_n^{t,\delta t}$ is defined as $A_n^{t,\delta t} = -i(2n-1)\delta t \int_0^1 H(t+x\delta t)P_{n-1}(x)dx$. Here, P_{n-1} denotes the shifted Legendre polynomials normalized to $(2n+1) \int_0^1 ds P_m(s)P_n(s) = \delta_{mn}$, and $A_n^{t,\delta t} \propto \delta t^n$. For a sufficiently small time interval δt , this Magnus expansion can be truncated at a finite order k , resulting in an approximation of $H_{[\infty]}$ as $H_{[k]} = i\delta t^{-1} \sum_{n=1}^k \Omega_n$.

Trotterization.—On real digital quantum devices, the exact time evolution operator $U(t+\delta t, t)$ for a smoothly varying Hamiltonian $H(t)$ is usually inaccessible. Thus, one needs to decompose the former into some elementary quantum gates using, e.g., Trotterization. For simplicity, we focus on the time dependence $H(t) = g(t)G + f(t)F$ with smooth functions $g(t)$ and $f(t)$, and two generic noncommuting Hermitian operators F and G . Let us assume that quantum devices admit the exact implementation of unitaries of the form $\exp(-iC_1G)$ or $\exp(-iC_2F)$ where $C_{1,2}$ are arbitrary real numbers; while the implementation of linear combinations of G and F , such as $\exp(-iC_1G - iC_2F)$, are not feasible.

We aim to approximate the target unitary operator up to a given order λ , such that $U(t+\delta t, t) = U_{[\lambda]}(t+\delta t, t) + \mathcal{O}(\delta t^\lambda)$. A larger λ leads to more accurate time evolution with smaller Trotter errors, but it also increases the circuit depth. The number of gates generally scales exponentially in λ , but better decompositions with fewer number of exponentials may exist [43]. In this work, we use $\lambda = 3$ and the approximation can be obtained by the second-order Trotter formula also known as the midpoint rule:

$$\begin{aligned} U_{[3]}(t+\delta t, t) &= \exp[-ig(t+\delta t/2)G\delta t/2] \\ &\quad \times \exp[-if(t+\delta t/2)F\delta t] \\ &\quad \times \exp[-ig(t+\delta t/2)G\delta t/2]. \end{aligned} \quad (2)$$

Adaptive algorithm.—The central concept of the adaptive algorithm is to maximize δt while ensuring that the measurement outcome of the expectation value and variance of $H_{[\infty]}$ remain within preset tolerances. However, $H_{[\infty]}$ is generically increasingly nonlocal as contributions of increasing order Ω_n are involved, introducing a significant measurement overhead. Therefore, depending on the measurement accuracy and efficiency, one may need to truncate $H_{[\infty]}$ to a finite order k to make the measurement procedure feasible on quantum computers [49–51]. Here, we consider a sufficiently large value for k , ensuring that errors in the piecewise conservation law are subdominant compared to the Trotter error. In the limit $\delta t \rightarrow 0$, this can be satisfied as long as $k \geq \lambda$; we prove it using perturbation theory, see Supplemental Material, Sec. 1 [52] for details.

Below, we first introduce a time local control scheme to adapt δt , which we find can involve severe heating effects. Then we propose a global control scheme to bound the accumulated errors and suppress heating.

In contrast to time independent systems where conserved energies solely depend on the initial state $|\psi(0)\rangle$, the

expectation values of $H_{[k]}$ for generic time dependent systems rely on the time evolved state $|\psi(t)\rangle$. As a result, there are no universal (in time) reference expectation values known *a priori* for the piecewise conserved Hamiltonians. Nonetheless, we can leverage the capability of quantum processors to measure the expectation values, $\mathcal{E}_i(t, \delta t) = \langle \psi(t) | H_{[k]} | \psi(t) \rangle / L$ with the system size L as a reasonable approximation to the conserved quantities for the true quantum state $|\phi(t)\rangle$. We maximize δt such that the time local error in the expectation value of $H_{[k]}$ remains below a threshold $d_\mathcal{E}$ [cf. Fig. 1(a)], i.e.,

$$|\mathcal{E}_f(t, \delta t) - \mathcal{E}_i(t, \delta t)| < d_\mathcal{E}, \quad (3)$$

where $\mathcal{E}_f(t, \delta t) = \langle \psi(t+\delta t) | H_{[k]} | \psi(t+\delta t) \rangle / L$ represents the expectation value of $H_{[k]}$ after the Trotterized evolution, given by $|\psi(t+\delta t)\rangle = U_{[\lambda]}(t, \delta t) |\psi(t)\rangle$. In the ideal case of $\lambda \rightarrow \infty$ and $k \rightarrow \infty$, we have $\mathcal{E}_f(t, \delta t) - \mathcal{E}_i(t, \delta t) = 0$ by definition. However, for any finite value of λ and k , this error does not vanish.

In addition, we also require the error in the variance to be bounded by the tolerance $d_{\delta\mathcal{E}^2}$, i.e., $|\delta\mathcal{E}_f^2(t, \delta t) - \delta\mathcal{E}_i^2(t, \delta t)| < d_{\delta\mathcal{E}^2}$, with

$$\begin{aligned} \delta\mathcal{E}_i^2(t, \delta t) &= L^{-1} \langle \psi(t) | H_{[k]}^2(t, \delta t) | \psi(t) \rangle - L\mathcal{E}_i^2, \\ \delta\mathcal{E}_f^2(t, \delta t) &= L^{-1} \langle \psi(t+\delta t) | H_{[k]}^2(t, \delta t) | \psi(t+\delta t) \rangle - L\mathcal{E}_f^2. \end{aligned} \quad (4)$$

According to the central limit theorem, constraining the errors in the lowest two moments of $H_{[k]}$ is sufficient to ensure the approximate conservation of its higher moments [33,53]. Therefore, the piecewise conservation of the Hamiltonian $H_{[k]}$ can be satisfied reasonably well, enabling reliable DQS of dynamics from time t to $t+\delta t$.

Note that Trotter errors can accumulate in the time evolved $|\psi(t)\rangle$, leading to deviations of \mathcal{E}_i and $\delta\mathcal{E}_i^2$ from the exact piecewise conservation laws. This effect is also present for time independent systems, where $H_{[k]}$ simplifies to a static Hamiltonian H . The energy constraint reduces to $|\langle \psi(t) | H | \psi(t) \rangle - \langle \psi(t+\delta t) | H | \psi(t+\delta t) \rangle| / L < d_\mathcal{E}$, which accumulates and cannot be bounded for long simulation times. Consequently, many-body systems tend to heat up and eventually become featureless. This Trotter-induced heating can be much more pronounced in time dependent systems, leading to unstable DQS of time evolution over long periods.

To address this challenge, we propose restrictions on the time global errors, representing the accumulation of all time local errors from previous steps:

$$\begin{aligned} \left| \sum_{n=1}^m [\mathcal{E}_f(t_n, \delta t_n) - \mathcal{E}_i(t_n, \delta t_n)] \right| &< d'_\mathcal{E}, \\ \left| \sum_{n=1}^m [\delta\mathcal{E}_f^2(t_n, \delta t_n) - \delta\mathcal{E}_i^2(t_n, \delta t_n)] \right| &< d'_{\delta\mathcal{E}^2}. \end{aligned} \quad (5)$$

These conditions imply the time local constraints, e.g., $|\mathcal{E}_f(t_m, \delta t_m) - \mathcal{E}_i(t_m, \delta t_m)| < 2d'_\mathcal{E}$ [54], but the converse is not true. Therefore, information from the past time steps is used to select the current step size, such that the algorithm is capable of automatically counteracting any accumulating Trotter-induced heating effects. This global control is necessary to handle the lack of energy conservation in time dependent systems.

We enforce these constraints via a feedback loop: initially, a large time step δt_m is chosen. We then measure \mathcal{E}_i and $\delta\mathcal{E}_i^2$ for the current quantum state $|\psi(t_m)\rangle$ and for the selected δt_m , as a prediction of the piecewise conserved quantities. We then implement the time evolution $U_{[\lambda]}(t_m, \delta t_m)$ on the quantum processor, yielding a candidate state $|\tilde{\psi}(t_m + \delta t_m)\rangle = U_{[\lambda]}(t_m, \delta t_m)|\psi(t_m)\rangle$. For this, we measure $\tilde{\mathcal{E}}_f$ and $\delta\tilde{\mathcal{E}}_f^2$. In case the measurement outcome violates the conditions of Eq. (5), a new smaller step size is proposed and the procedure restarts.

We use the bisection search method to find a new suitable δt_m . This can be efficiently implemented with a few trials whose number does not scale with system size and the truncation order k , cf. Ref. [33] and Supplemental Material, Sec. 3. [52] The extra measurement cost only depends polynomially on the system size and can be further improved to logarithmic dependence by using classical shadows [55–57]. Once a suitable δt_m has been found, we obtain the state $|\psi(t_m + \delta t_m)\rangle$ at the next time, and repeat the procedure.

Numerical simulation.—We next numerically compare local and global constraint schemes and find better performance of tADA-Trotter with time global control.

Although this algorithm is applicable to various models and initial states, for concreteness, we start from a product state $|\psi(0)\rangle = \exp(-i\theta \sum_j \sigma_j^x) |\downarrow \dots \downarrow\rangle$ and a nonintegrable quantum Ising model, with Hamiltonian $H(t) = g(t)H_x + f(t)H_z$ with $H_z = J_z \sum_j \sigma_j^z \sigma_{j+1}^z + h_z \sum_j \sigma_j^z$, $H_x = h_x \sum_j \sigma_j^x$, where σ_j^x and σ_j^z are Pauli matrices acting on site j of a chain consisting of L sites with periodic boundary conditions. We consider a uniform coupling J_z , and transverse and longitudinal fields h_x and h_z , respectively.

We choose a static longitudinal field $f(t) = 1$ and an oscillating transverse field $g(t) = \cos(\omega t) \exp(-t/\tau) + 1$ with nonzero mean, frequency ω , and exponentially decaying amplitude. For $t \gg \tau$, the system becomes effectively time independent. Hence, this protocol contains different timescales and thus provides an ideal testbed for our algorithm. We employ Eq. (2) to implement the Trotterized dynamics and truncate the piecewise conserved Hamiltonian to $H_{[k]}$ with $k = 5$.

In Fig. 2, we depict the expectation value of $H_{[k]}$ with the local and global control schemes. The exact solution varies at early times and becomes static at later times as expected. The predicted conserved value \mathcal{E}_i at early times closely follows the exact solution. The expectation value \mathcal{E}_f after

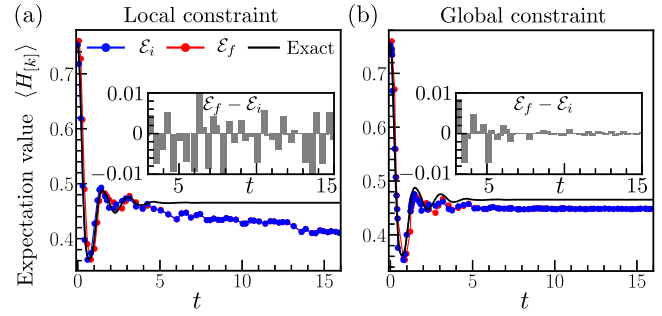


FIG. 2. Comparison between the time local and global constraint. (a) Local constraint with tolerances $d_\mathcal{E} = 0.01$, $d_{\delta\mathcal{E}^2} = 0.02$, and $d'_\mathcal{E} = d'_{\delta\mathcal{E}^2} = \infty$. (b) Time global errors are bounded, with the tolerance $d_\mathcal{E} = d_{\delta\mathcal{E}^2} = \infty$, $d'_\mathcal{E} = 0.01$, $d'_{\delta\mathcal{E}^2} = 0.02$. The following Hamiltonian parameters are used for numerical simulation, $J_z = 1$, $h_x = 1$, $h_z = 0.5$, $\tau = 1$, $\omega = 4$, $L = 16$, $\theta = 2$.

implementing the Trotterized dynamics deviates from \mathcal{E}_i very weakly in both cases.

A crucial difference occurs at later times. In Fig. 2(a), for $t > 5$ in units of the Ising coupling J_z , the predicted value \mathcal{E}_i exhibits a noticeable drift toward zero, indicating the accumulation of Trotter errors. Note, this Trotter-induced heating is not the same as the energy nonconservation that goes along with $H(t)$ [36–38]. It happens because statistically, a stepsize increasing the system’s entropy is more likely. To emphasize this point, we plot the time local error $\mathcal{E}_f(t_n, \delta t_n) - \mathcal{E}_i(t_n, \delta t_n)$ at each time, and clearly, δt is chosen in a way that negative values appear more frequently. By contrast, when constraining the global errors according to Eq. (5), this deviation approximately centers around zero, indicating better controlled heating. Consequently, the overall drift in \mathcal{E}_i is suppressed. For a specific time t_0 , as long as $t_0 \gg \tau$ where the system becomes effectively time independent, one can show that $\mathcal{E}_f(t_m, \delta t_m) = \mathcal{E}_i(t_{m+1}, \delta t_{m+1})$ for any $t_m \geq t_0$. Hence, Eq. (5) reduces to $|\mathcal{E}_i(t_m, \delta t_m) - \mathcal{E}_i(t_0, \delta t_0)| < d'_\mathcal{E}$, strictly prohibiting the overall drift at long times as shown in Fig. 2(b).

Controlling errors in the expectation values of $H_{[k]}$ ensures accurate DQS of local observables. Fig. 3 shows

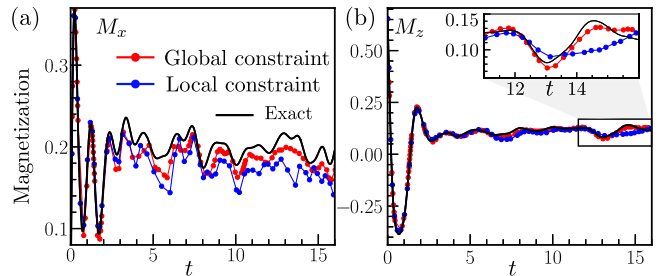


FIG. 3. Global constraint leads to more stable simulation results than local constraint. Magnetization in x (a) and z (b) direction. We use the same parameters as in Fig. 2. The inset shows details of the dynamics in a small time window.

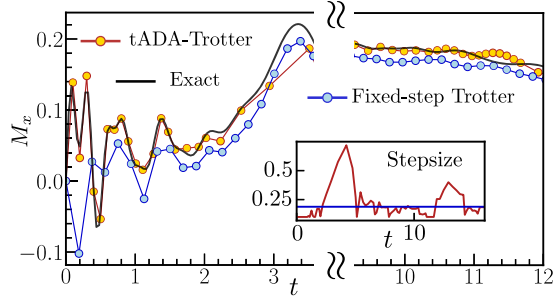


FIG. 4. Comparison between tADA-Trotter and fixed-step Trotter algorithms. Inset depicts the stepsize that varies in time. It takes larger values when external driving fields are weak. We use the following Hamiltonian parameters for numerical simulation, $J_z = 1$, $h_x = 3$, $h_z = 0.5$, $\tau = 30$, $\omega = 0.8$, $L = 18$, $\theta = 2$, $d'_E = 0.03$, $d'_{\delta E^2} = 0.1$.

the magnetizations $M_\alpha = \sum_j \sigma_j^\alpha / L$ for $\alpha = x, z$, demonstrating that global constraint generally yields a more accurate simulation compared to the local constraint. In particular, in Fig. 3(a) with the local constraint, significant errors arise for $t > 5$. It corresponds to the time when notable deviation arises in the piecewise conserved quantities as shown in Fig. 2(a). In contrast, the globally constrained data closely follows the exact solution for an extended period.

We now demonstrate that by constraining the time global errors, tADA-Trotter achieves superior simulation precision compared to the fixed-step Trotter when the same total simulation time is reached. In the field $x(t)$ we select a driving frequency $\omega = 0.8$ that is comparable to other local energy scales in the system. The characteristic decay timescale is chosen as $\tau = 30$. With a total number of Trotter steps $N = 100$, the achievable simulation time is approximately $t \sim 20$, during which the significant time dependence in the Hamiltonian is still present.

In Fig. 4, $M_x = \sum_j \sigma_j^x / L$ is depicted with orange circles, which closely reproduces the exact solution (black). Simulation errors only become visible at later times, e.g., $t_m > 11$. In contrast, the fixed-step Trotter ($\delta t_m = 0.2$) already introduces substantial errors in the magnetization within a short time. The Trotter step size (Fig. 4 inset) fluctuates within approximately one order of magnitude $\delta t_m \in [0.1, 0.7]$, highlighting the advantage and the flexibility of tADA-Trotter. Particularly, at early times, when the quantum state undergoes rapid changes under a strong driving field, smaller step sizes are employed ($\delta t_m \approx 0.1$). Conversely, when the driving $g(t)$ has relatively smaller values around $t_m \approx 4$ and 12, the step size automatically increases to $\delta t \approx 0.7$ and 0.4, respectively.

The time global errors, Fig. 5, remain bounded below the specified thresholds for the majority of the time evolution. However, it should be noted that due to the tight tolerances at early times, the accumulated errors in the piecewise conserved quantities may occasionally exceed the bounds.

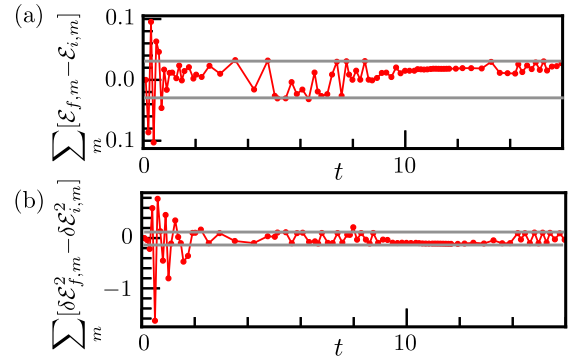


FIG. 5. Time global errors under the global constraint in the expectation value and variance of $H_{[k]}$. Errors are bounded for most of the time evolution. Same parameters as in Fig. 4.

This phenomenon can also cause the tADA-Trotter to “freeze,” wherein it tends to select the smallest possible step size, which in this case is set to 0.1.

Discussion.—We have introduced the concept of piecewise conserved quantities and combined it with a time global error constraint to devise an adaptive Trotterization scheme to enable reliable DQS of generic time dependent Hamiltonians. In the presence of weak hardware noise, we expect that tADA-Trotter remains robust and can even self-correct the dissipation-induced errors [58]. We estimate that the shot overhead for a single step is around 10^4 , which can be efficiently implemented on current quantum processors with fast gate implementation, cf. Supplemental Material, Sec. 3 [52].

In a specific example, we demonstrate the superior performance of tADA-Trotter compared to the fixed-step Trotter method. The intricate interplay between external driving and quantum thermalization can result in highly complex many-body dynamics [59–62]. Therefore, for future investigations, conducting a systematic benchmark of various algorithms across different models, initial states, and time dependence would be of great value, as would be a comparison against higher-order truncation schemes.

Furthermore, the extension of piecewise conservation laws to open quantum systems to enable adaptive Trotter step sizes represents an intriguing open question [63–66]. Additionally, considering the widespread use of Trotterization in classical numerical algorithms such as the time evolving block decimation method, the application of tADA-Trotter to enhance the efficiency and accuracy of these methods holds significant potential.

Note added.—We recently became aware of a relevant work exploring another adaptive algorithm for DQS of time evolution [45].

We thank T. Ikeda for enlightening discussions. This work is supported by “The Fundamental Research Funds for the Central Universities, Peking University,” and by

“High-performance Computing Platform of Peking University” and the Deutsche Forschungsgemeinschaft under cluster of excellence ct.qmat (EXC 2147, Project No. 390858490). This project has received funding from the European Research Council (ERC) under the European Unions Horizon 2020 research and innovation programme (Grant Agreement No. 853443). M. B. was supported in part by the International Centre for Theoretical Sciences (ICTS) for participating in the program—Periodically and quasi-periodically driven complex systems (code: ICTS/pdcs2023/6).

* Contact author: hzhao@pku.edu.cn

- [1] I. M. Georgescu, S. Ashhab, and F. Nori, Quantum simulation, *Rev. Mod. Phys.* **86**, 153 (2014).
- [2] J. Preskill, Quantum computing in the NISQ era and beyond, *Quantum* **2**, 79 (2018).
- [3] R. Blatt and C. F. Roos, Quantum simulations with trapped ions, *Nat. Phys.* **8**, 277 (2012).
- [4] C. Monroe, W. C. Campbell, L.-M. Duan, Z.-X. Gong, A. V. Gorshkov, P. Hess, R. Islam, K. Kim, N. M. Linke, G. Pagano *et al.*, Programmable quantum simulations of spin systems with trapped ions, *Rev. Mod. Phys.* **93**, 025001 (2021).
- [5] P. T. Dumitrescu, J. G. Bohnet, J. P. Gaebler, A. Hankin, D. Hayes, A. Kumar, B. Neyenhuis, R. Vasseur, and A. C. Potter, Dynamical topological phase realized in a trapped-ion quantum simulator, *Nature (London)* **607**, 463 (2022).
- [6] Y. Salathé, M. Mondal, M. Oppliger, J. Heinsoo, P. Kurpiers, A. Potočnik, A. Mezzacapo, U. Las Heras, L. Lamata, E. Solano *et al.*, Digital quantum simulation of spin models with circuit quantum electrodynamics, *Phys. Rev. X* **5**, 021027 (2015).
- [7] K. Satzinger, Y.-J. Liu, A. Smith, C. Knapp, M. Newman, C. Jones, Z. Chen, C. Quintana, X. Mi, A. Dunsworth *et al.*, Realizing topologically ordered states on a quantum processor, *Science* **374**, 1237 (2021).
- [8] J. Dborin, V. Wimalaweera, F. Barratt, E. Ostby, T. E. O’Brien, and A. G. Green, Simulating groundstate and dynamical quantum phase transitions on a superconducting quantum computer, *Nat. Commun.* **13**, 5977 (2022).
- [9] S. Moses, C. Baldwin, M. Allman, R. Ancona, L. Ascarrunz, C. Barnes, J. Bartolotta, B. Bjork, P. Blanchard, M. Bohn *et al.*, A race track trapped-ion quantum processor, *Phys. Rev. X* **13**, 041052 (2023).
- [10] C. Chen, G. Bornet, M. Bintz, G. Emperauger, L. Leclerc, V. S. Liu, P. Scholl, D. Barredo, J. Hauschild, S. Chatterjee *et al.*, Continuous symmetry breaking in a two-dimensional rydberg array, *Nature (London)* **616**, 691 (2023).
- [11] Y. Kim, A. Eddins, S. Anand, K. X. Wei, E. Van Den Berg, S. Rosenblatt, H. Nayfeh, Y. Wu, M. Zaletel, K. Temme *et al.*, Evidence for the utility of quantum computing before fault tolerance, *Nature (London)* **618**, 500 (2023).
- [12] M. Suzuki, General theory of fractal path integrals with applications to many-body theories and statistical physics, *J. Math. Phys. (N.Y.)* **32**, 400 (1991).
- [13] D. W. Berry, G. Ahokas, R. Cleve, and B. C. Sanders, Efficient quantum algorithms for simulating sparse Hamiltonians, *Commun. Math. Phys.* **270**, 359 (2007).
- [14] D. Poulin, M. B. Hastings, D. Wecker, N. Wiebe, A. C. Doherty, and M. Troyer, The Trotter step size required for accurate quantum simulation of quantum chemistry, [arXiv:1406.4920](https://arxiv.org/abs/1406.4920).
- [15] R. Babbush, D. W. Berry, I. D. Kivlichan, A. Y. Wei, P. J. Love, and A. Aspuru-Guzik, Exponentially more precise quantum simulation of fermions in second quantization, *New J. Phys.* **18**, 033032 (2016).
- [16] M. Heyl, P. Hauke, and P. Zoller, Quantum localization bounds Trotter errors in digital quantum simulation, *Sci. Adv.* **5**, eaau8342 (2019).
- [17] A. Tranter, P. J. Love, F. Mintert, N. Wiebe, and P. V. Coveney, Ordering of Trotterization: Impact on errors in quantum simulation of electronic structure, *Entropy* **21**, 1218 (2019).
- [18] C. Cirstoiu, Z. Holmes, J. Iosue, L. Cincio, P. J. Coles, and A. Sornborger, Variational fast forwarding for quantum simulation beyond the coherence time, *npj Quantum Inf.* **6**, 1 (2020).
- [19] A. Bolens and M. Heyl, Reinforcement learning for digital quantum simulation, *Phys. Rev. Lett.* **127**, 110502 (2021).
- [20] Y.-X. Yao, N. Gomes, F. Zhang, C.-Z. Wang, K.-M. Ho, T. Iadecola, and P. P. Orth, Adaptive variational quantum dynamics simulations, *PRX Quantum* **2**, 030307 (2021).
- [21] S.-H. Lin, R. Dilip, A. G. Green, A. Smith, and F. Pollmann, Real-and imaginary-time evolution with compressed quantum circuits, *PRX Quantum* **2**, 010342 (2021).
- [22] J. Richter and A. Pal, Simulating hydrodynamics on noisy intermediate-scale quantum devices with random circuits, *Phys. Rev. Lett.* **126**, 230501 (2021).
- [23] R. Mansuroglu, T. Eckstein, L. Nützel, S. A. Wilkinson, and M. J. Hartmann, Variational Hamiltonian simulation for translational invariant systems via classical pre-processing, *Quantum Sci. Technol.* **8**, 025006 (2023).
- [24] C. M. Keever and M. Lubasch, Classically optimized Hamiltonian simulation, *Phys. Rev. Res.* **5**, 023146 (2023).
- [25] L. Pastori, T. Olsacher, C. Kokail, and P. Zoller, Characterization and verification of Trotterized digital quantum simulation via Hamiltonian and Liouvillian learning, *PRX Quantum* **3**, 030324 (2022).
- [26] M. S. Tepaske, D. Hahn, and D. J. Luitz, Optimal compression of quantum many-body time evolution operators into brickwall circuits, *SciPost Phys.* **14**, 073 (2023).
- [27] Z.-J. Zhang, J. Sun, X. Yuan, and M.-H. Yung, Low-depth Hamiltonian simulation by an adaptive product formula, *Phys. Rev. Lett.* **130**, 040601 (2023).
- [28] R. Mansuroglu, F. Fischer, and M. J. Hartmann, Problem specific classical optimization of Hamiltonian simulation, *Phys. Rev. Res.* **5**, 043035 (2023).
- [29] E. Granet and H. Dreyer, Continuous Hamiltonian dynamics on noisy digital quantum computers without Trotter error, [arXiv:2308.03694](https://arxiv.org/abs/2308.03694).
- [30] L. Postler and S. Heußen, I. Pogorelov, M. Rispler, T. Feldker, M. Meth, C. D. Marciniak, R. Stricker, M. Ringbauer, R. Blatt *et al.*, Demonstration of fault-tolerant

- universal quantum gate operations, *Nature (London)* **605**, 675 (2022).
- [31] S. Krinner, N. Lacroix, A. Remm, A. Di Paolo, E. Genois, C. Leroux, C. Hellings, S. Lazar, F. Swiadek, J. Herrmann *et al.*, Realizing repeated quantum error correction in a distance-three surface code, *Nature (London)* **605**, 669 (2022).
- [32] E. H. Chen, T. J. Yoder, Y. Kim, N. Sundaresan, S. Srinivasan, M. Li, A. D. Córcoles, A. W. Cross, and M. Takita, Calibrated decoders for experimental quantum error correction, *Phys. Rev. Lett.* **128**, 110504 (2022).
- [33] H. Zhao, M. Bukov, M. Heyl, and R. Moessner, Making Trotterization adaptive and energy-self-correcting for NISQ devices and beyond, *PRX Quantum* **4**, 030319 (2023).
- [34] L. D'Alessio, Y. Kafri, A. Polkovnikov, and M. Rigol, From quantum chaos and eigenstate thermalization to statistical mechanics and thermodynamics, *Adv. Phys.* **65**, 239 (2016).
- [35] D. A. Abanin, E. Altman, I. Bloch, and M. Serbyn, Colloquium: Many-body localization, thermalization, and entanglement, *Rev. Mod. Phys.* **91**, 021001 (2019).
- [36] A. Lazarides, A. Das, and R. Moessner, Equilibrium states of generic quantum systems subject to periodic driving, *Phys. Rev. E* **90**, 012110 (2014).
- [37] D. A. Abanin, W. De Roeck, and F. H. Lüscher, Exponentially slow heating in periodically driven many-body systems, *Phys. Rev. Lett.* **115**, 256803 (2015).
- [38] T. Kuwahara, T. Mori, and K. Saito, Floquet–magnus theory and generic transient dynamics in periodically driven many-body quantum systems, *Ann. Phys. (Amsterdam)* **367**, 96 (2016).
- [39] D. Poulin, A. Qarry, R. Somma, and F. Verstraete, Quantum simulation of time-dependent Hamiltonians and the convenient illusion of hilbert space, *Phys. Rev. Lett.* **106**, 170501 (2011).
- [40] Y.-H. Chen, A. Kalev, and I. Hen, Quantum algorithm for time-dependent Hamiltonian simulation by permutation expansion, *PRX Quantum* **2**, 030342 (2021).
- [41] J. W. Z. Lau, K. Bharti, T. Haug, and L. C. Kwek, Noisy intermediate scale quantum simulation of time dependent Hamiltonians, *arXiv:2101.07677*.
- [42] J. Watkins, N. Wiebe, A. Roggero, and D. Lee, Time-dependent Hamiltonian simulation using discrete clock constructions, *arXiv:2203.11353*.
- [43] T. N. Ikeda, A. Abrar, I. L. Chuang, and S. Sugiura, Minimum fourth-order Trotterization formula for a time-dependent Hamiltonian, *Quantum* **7**, 1168 (2023).
- [44] D. An, D. Fang, and L. Lin, Time-dependent Hamiltonian simulation of highly oscillatory dynamics and superconvergence for Schrödinger equation, *Quantum* **6**, 690 (2022).
- [45] T. N. Ikeda and K. Fujii, Trotter24: A precision-guaranteed adaptive stepsize Trotterization for Hamiltonian simulations, *arXiv:2307.05406*.
- [46] L. K. Kovalsky, F. A. Calderon-Vargas, M. D. Grace, A. B. Magann, J. B. Larsen, A. D. Baczewski, and M. Sarovar, Self-healing of Trotter error in digital adiabatic state preparation, *Phys. Rev. Lett.* **131**, 060602 (2023).
- [47] M. Hochbruck and C. Lubich, On magnus integrators for time-dependent Schrödinger equations, *SIAM J. Numer. Anal.* **41**, 945 (2003).
- [48] A. Alvermann and H. Fehske, High-order commutator-free exponential time-propagation of driven quantum systems, *J. Comput. Phys.* **230**, 5930 (2011).
- [49] C. Kokail, C. Maier, R. van Bijnen, T. Brydges, M. K. Joshi, P. Jurcevic, C. A. Muschik, P. Silvi, R. Blatt, C. F. Roos *et al.*, Self-verifying variational quantum simulation of lattice models, *Nature (London)* **569**, 355 (2019).
- [50] X. Mi, P. Roushan, C. Quintana, S. Mandra, J. Marshall, C. Neill, F. Arute, K. Arya, J. Atalaya, R. Babbush *et al.*, Information scrambling in quantum circuits, *Science* **374**, 1479 (2021).
- [51] P. Naldesi, A. Elben, A. Minguzzi, D. Clément, P. Zoller, and B. Vermersch, Fermionic correlation functions from randomized measurements in programmable atomic quantum devices, *Phys. Rev. Lett.* **131**, 060601 (2023).
- [52] See Supplemental Material at <http://link.aps.org/supplemental/10.1103/PhysRevLett.133.010603> for detailed perturbative analysis of errors and more numerical simulation, as well as discussion regarding the extra costs in running adaptive algorithms.
- [53] M. Hartmann, G. Mahler, and O. Hess, Gaussian quantum fluctuations in interacting many particle systems, *Lett. Math. Phys.* **68**, 103 (2004).
- [54] To show this, we define $\Delta_{m-1} = \sum_{n=1}^{m-1} \mathcal{E}_f(t_n, \delta t_n) - \mathcal{E}_i(t_n, \delta t_n)$, which satisfies $-d'_\mathcal{E} < \Delta_{m-1} < d'_\mathcal{E}$ with a positive $d'_\mathcal{E}$. For the next step, one has $-d'_\mathcal{E} < \Delta_{m-1} + \mathcal{E}_f(t_m, \delta t_m) - \mathcal{E}_i(t_m, \delta t_m) < d'_\mathcal{E}$, leading to $-2d'_\mathcal{E} < \mathcal{E}_f(t_m, \delta t_m) - \mathcal{E}_i(t_m, \delta t_m) < 2d'_\mathcal{E}$.
- [55] H.-Y. Huang, R. Kueng, and J. Preskill, Predicting many properties of a quantum system from very few measurements, *Nat. Phys.* **16**, 1050 (2020).
- [56] H.-Y. Huang, R. Kueng, and J. Preskill, Efficient estimation of Pauli observables by derandomization, *Phys. Rev. Lett.* **127**, 030503 (2021).
- [57] A. Elben, S. T. Flammia, H.-Y. Huang, R. Kueng, J. Preskill, B. Vermersch, and P. Zoller, The randomized measurement toolbox, *Nat. Rev. Phys.* **5**, 9 (2023).
- [58] We have explicitly demonstrated this for a time independent Hamiltonian in Ref. [33].
- [59] M. Kolodrubetz, D. Sels, P. Mehta, and A. Polkovnikov, Geometry and non-adiabatic response in quantum and classical systems, *Phys. Rep.* **697**, 1 (2017).
- [60] S. Sugiura, P. W. Claeys, A. Dymarsky, and A. Polkovnikov, Adiabatic landscape and optimal paths in ergodic systems, *Phys. Rev. Res.* **3**, 013102 (2021).
- [61] A. De La Torre, D. M. Kennes, M. Claassen, S. Gerber, J. W. McIver, and M. A. Sentef, Colloquium: Nonthermal pathways to ultrafast control in quantum materials, *Rev. Mod. Phys.* **93**, 041002 (2021).
- [62] W. W. Ho, T. Mori, D. A. Abanin, and E. G. Dalla Torre, Quantum and classical floquet prethermalization, *Ann. Phys. (Amsterdam)* **454**, 169297 (2023).
- [63] J. Han, W. Cai, L. Hu, X. Mu, Y. Ma, Y. Xu, W. Wang, H. Wang, Y. Song, C.-L. Zou *et al.*, Experimental simulation of open quantum system dynamics via Trotterization, *Phys. Rev. Lett.* **127**, 020504 (2021).

- [64] W. A. de Jong, M. Metcalf, J. Mulligan, M. Płoskoń, F. Ringer, and X. Yao, Quantum simulation of open quantum systems in heavy-ion collisions, *Phys. Rev. D* **104**, L051501 (2021).
- [65] H. Kamakari, S.-N. Sun, M. Motta, and A. J. Minnich, Digital quantum simulation of open quantum systems using quantum imaginary-time evolution, *PRX Quantum* **3**, 010320 (2022).
- [66] T. Vovk and H. Pichler, Entanglement-optimal trajectories of many-body quantum Markov processes, *Phys. Rev. Lett.* **128**, 243601 (2022).